PHYSICAL REVIEW B VOLUME 18, NUMBER 9 1 NOVEMBER 1978

Phonon-induced diffuse x-ray scattering in β-AgI

H. U. Beyeler, P. Brüesch, and T. Hibma
Brown Boveri Research Center, 5405 Baden-Dättwil, Switzerland

W. Bührer
Institut für Reaktortechnik Eidgenössische Technische Hochschule Zürich, c/o Eidgenössisches Institut für Reaktortorschung, 5303 Würenligen, Switzerland

(Received 19 June 1978)

The one-phonon diffuse x-ray scattering of β-AgI has been computed from a lattice-dynamical model with parameters derived from neutron scattering data. The computed diffuse scattering is compared to experimental results and excellent agreement is found. The complex and intense diffuse scattering of the ordered β phase originates from a band of low-frequency dispersionless lattice modes. There are strong indications for the existence of similar low-frequency dispersionless (local) lattice excitations in the disordered α phase of AgI. Thus we argue that the diffuse x-ray scattering of the α phase is to a large extent of thermal origin, and that intense phonon-induced x-ray scattering may in certain superionic conductors completely preclude the extraction of information about static short-range order from diffuse x-ray scattering.

I. INTRODUCTION

Since the early days of x-ray investigations the study of diffuse scattering has been recognized as a powerful tool to obtain detailed information on the static and dynamical properties of solids. Apart from the incoherent Compton scattering the diffuse scattering is directly related to the time-averaged electron density-density correlation within the sample. In general this correlation contains contributions from density fluctuations due to lattice vibrations and from static disorder. The cross section for first-order phonon scattering processes is inversely proportional to the frequency of the scattering lattice vibration. In an ordinary solid the main thermal contributions are thus originating from the long-wavelength acoustical phonons resulting in diffuse "thermal haloes" around Bragg reflexions. Already in 1925 Waller[1] realized that under certain conditions thermal diffuse scattering may also produce an appreciable intensity far from Bragg reflexions, a fact first experimentally confirmed in 1938 by Laval.[2] For a review of the early work in that field the reader is referred to Ref. 3.

Unfortunately the relationship between thermal diffuse scattering and the relevant lattice-dynamical parameters is generally very complex so that when the more powerful neutron scattering technique became available the interest in the experimental study of thermal diffuse x-ray scattering rapidly declined.

On the other hand diffuse x-ray study is a widely used tool for the investigation of short-range order in disordered solids,[4-7] superstructures due to lattice instabilities,[8,9] and of ion-ion correlations in superionic conductors.[10-16]

In such experiments the presence of thermal diffuse scattering remains a constant potential complication as one is generally unable to account quantitatively for the phonon-induced scattering. In this work we present for the first time a detailed analysis of the thermal diffuse scattering of β-AgI, a compound with a very peculiar phonon structure and show how low-frequency lattice modes may result in very intense structured diffuse scattering through the whole reciprocal space. The results are of particular relevance for the interpretation of diffuse scattering data in superionic conductors.

II. DIFFUSE SCATTERING IN SUPERIONIC CONDUCTORS

Superionic conductors or solid electrolytes constitute a particularly interesting class of partially disordered systems. They consist of an ordered framework structure and a disordered sublattice of mobile ions.[17] Each of the latter disposes in general of more than one equivalent lattice site. The interaction between the mobile ions imposes a certain degree of short-range order on the sublattice of the mobile ions. As a consequence the probability for a diffusional jump of a particular ion depends on the configuration of the neighboring ions, an effect sometimes accounted for in terms of a configurational energy contribution to the jump activation energy. As calculations show, such effects may drastically lower the effective diffusion barriers[18,19] and thus be of prime importance for a microscopic understanding of the conduction mechanism.

Information on ion-ion correlations and domain formation in superionic conductors has been extracted from diffuse x-ray data without explicitly

accounting for thermal scattering of the generally very complex structures. There is, however, evidence that at least some of these materials exhibit unusual low-frequency lattice modes[20-22] which in turn may be the origin of intense thermal diffuse scattering. As shown in Sec. III silver iodide offers a unique opportunity to study this question in detail.

III. SILVER IODIDE

At room temperature silver iodide crystallizes in an ordered hexagonal (Wurtzite) structure[23] (β-AgI). The lattice dynamics of this phase has been investigated by inelastic neutron scattering experiments[24,25] which were interpreted in terms of a valence shell model. As a pecularity β-AgI displays almost dispersionless low-frequency lattice modes resulting in a very marked peak in the density of states around 20 cm^{-1}.

At 146 °C silver iodide transforms to the disordered α phase in which the iodine ions form a regular bcc lattice whereas the silver ions are highly mobile and each one disposes of six tetrahedral sites.[26-28] Although the $\beta \rightarrow \alpha$ transition is of first order the interatomic distances do not change much and one may speculate that in zeroth order the lattice dynamics of α-AgI is not too different from that of β-AgI. This conjecture is supported by the calculations of Alben *et al.* and by recent inelastic neutron scattering experiments, which both evidence a large density of state at low frequencies, reminiscent of the low-frequency modes found in the β phase. We may thus conclude that β-AgI exhibits a low-frequency phonon-induced diffuse scattering that is representative of the thermal diffuse scattering of the superionic conductor α-AgI but with no additional diffuse scattering due to static disorder. Experimentally β-AgI displays a rich diffuse scattering pattern [see Fig. 1(a)] not differing in intensity or complexity from other superionic conductors such as $HgAg_2I_4$,[12] or $(C_5H_5NH)Ag_5I_6$.[29]

IV. COMPUTATION OF THE PHONON-INDUCED DIFFUSE SCATTERING

As we have at our disposal a complete lattice-dynamical model of β-AgI yielding phonon eigenfrequencies $\omega(\vec{q})$ and eigenvectors $\vec{e}(\kappa|\vec{q},j)$ for all branches j and phonon vectors $\vec{q}$ (κ numbers the atoms in the unit cell) we may compute the corresponding diffuse scattering and by comparison verify whether the observed scattering agrees with the scattering derived from the model. The model parameters were completely determined from neutron scattering data so there is no adjustable parameter involved in this procedure.

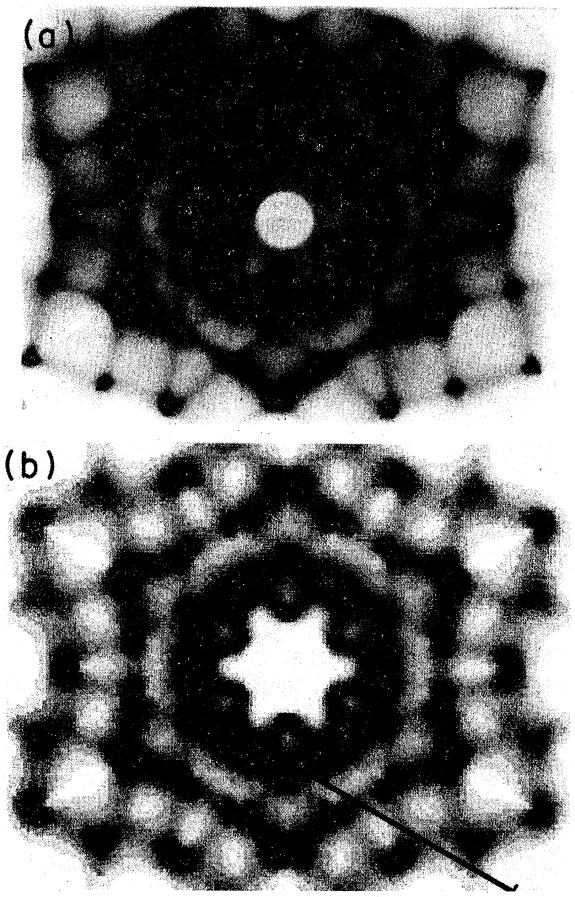

FIG. 1. (a) (Top) experimental diffuse scattering in β-AgI. The picture is taken in a steady-crystal–steady-film geometry (monochromatic *Laue* set up) with the incident beam perpendicular to the hexagonal basal plane. The scattering intensity thus corresponds to that on a sphere tangential to the reciprocal basal plane [(001) Ewald sphere] as shown in Fig. 5. The scattering on the trace in the lower left side is analyzed in Fig. 6. (b) (Bottom) Computed thermal diffuse scattering intensity in the geometry of Fig. 1(a). The scattering is displayed on a 16-step gray scale. The data are corrected for absorption according to the experimental situation of Fig. 1(a).

The one-phonon scattering intensity at the point $\vec{Q}$ in reciprocal space is given by[3,30]

$$I(\vec{Q}) = N \sum_j \frac{Q^2 |G_j(\vec{Q})|^2 E(\vec{q},j)}{m \omega_j^2(\vec{q})} , \tag{1}$$

where the "phonon scattering factor" QG_j is

$$QG_j(\vec{Q}) = \sqrt{m}\,\vec{Q} \sum_\kappa \frac{\vec{e}(\kappa|\vec{q},j)}{\sqrt{m_\kappa}} f_\kappa(Q) \times \exp[-W_\kappa(Q)] \exp[i\vec{g}\vec{r}(\kappa)] . \tag{2}$$

N is the total number of unit cells, $m = \sum m_\kappa$ the total mass of one unit cell, f_κ the scattering fac-

tor of atom κ, W_κ its Debye-Waller factor, r_κ its position within the unit cell, $\vec{g}$ is the reciprocal lattice vector closest to $\vec{Q}$ so that

$$\vec{Q}=\vec{g}+\vec{q}\ . \tag{3}$$

$\vec{E}(\vec{q},j)$ is the total energy of the phonons $(\vec{q},j)$:

$$E(\vec{q},j)=\hbar\omega_j(\vec{q})\left(\frac{1}{\exp[\hbar\omega_j(\vec{q})/kT]-1}+\frac{1}{2}\right). \tag{4}$$

For the actual computation we proceeded as follows: for each given $\vec{Q}$ the corresponding $\vec{q}$ and the respective phonon frequencies and vectors were determined, then finally the diffuse scattering of each phonon branch j at this point was computed according to Eq. (1).

The full spacial dependence of the diffuse scattering in reciprocal space represents a very large body of data. It is not the aim of this work to perform any numerical comparison between computed and measured scattering intensity; this would involve explicit accounting for scattering in air, incoherent scattering, absorption, etc. Instead we confine ourselves to a visual comparison of the structures in the computed and the experimental diffuse scattering. In order to facilitate this comparison we have included an approximate absorption correction in the computed results. This results in an overall decrease of the computed intensity comparable to that of the experimental pictures but does in no way alter the structural features of the diffuse scattering. We present the computed intensities in terms of a 16-step shade scale plotted with a Varian electrostatic computer plotter.

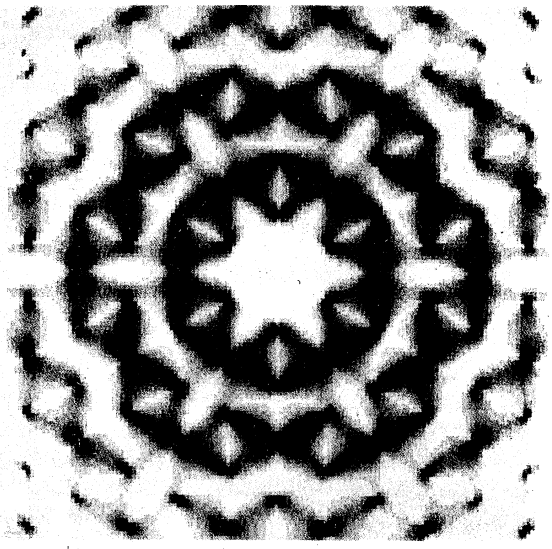

FIG. 2. Computed thermal diffuse scattering in the reciprocal basal plane of β-AgI. The data do not contain the (infinitely sharp) Bragg reflexions, but their position is evidenced by the diffuse haloes due to the long-wavelength acoustical phonons.

V. COMPARISON OF COMPUTED AND EXPERIMENTAL DIFFUSE SCATTERING

The computed intensities in the hexagonal basal plane in reciprocal space are shown in Fig. 2. The computation does not include the (infinitely sharp) Bragg reflexions but their position is evident from the thermal diffuse haloes around the Bragg spots due to the long-wavelength acoustical phonons. In addition to this "normal" thermal scattering there are diffuse streaks, connecting certain Bragg spots, overall a very complex diffuse intensity distribution. The same remarks apply to the computed intensity in the $(1\bar{1}0)$ plane shown in Fig. 3. As shown later in detail the extended diffuse structures originate from the dispersionless lattice modes around 20 cm^{-1}; the contribution of the optical modes is negligible.

Experimentally we have investigated the diffuse scattering on single crystal β-AgI using a fixed crystal fixed film method. A doubly bent LiF crystal served as monochromator for the Mo $K\alpha$ radiation. In this arrangement the intensity on a plane film represents the projection of a spherical cut through the reciprocal space. The single crystals had been grown from an aqueous solution and were annealed for several days slightly below 146 °C in order to obtain samples free of polytypes. The samples were either thin cleaved plates (for incident beam parallel to hexagonal axis) or

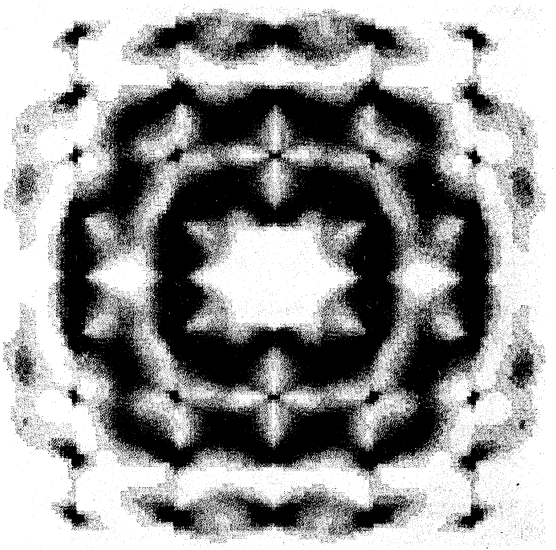

FIG. 3. Computed thermal diffuse scattering in the reciprocal $(1\bar{1}0)$ plane.

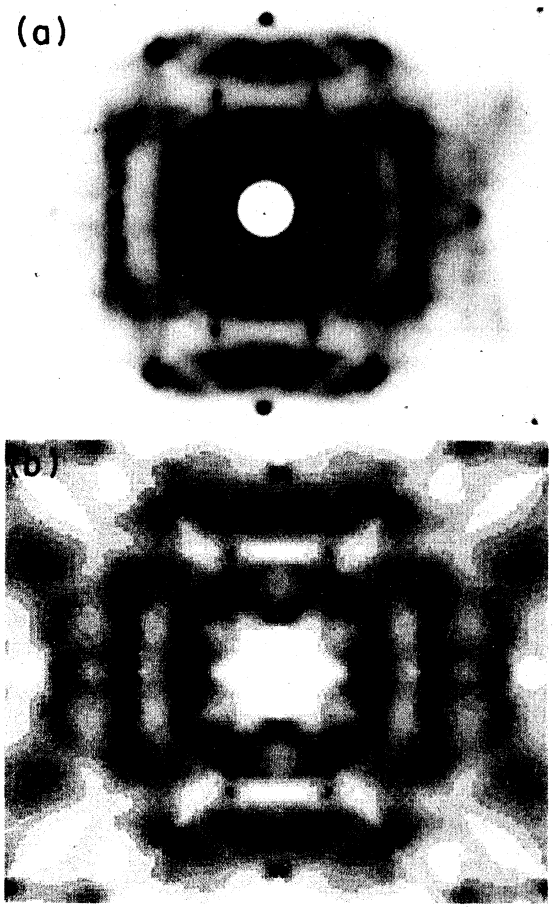

FIG. 4. (a) (Top) Experimental diffuse scattering on a sphere tangential to the reciprocal $(1\bar{1}0)$ plane [$(1\bar{1}0)$ Ewald sphere]; as thin rodlike samples had to be used in this geometry, the central part of the picture contains an appreciable amount of air scattering from the primary beam. (b) (Bottom) Computed thermal diffuse scattering in the geometry of Fig. 4(a).

thin etched rods (for the other geometries). All presented results were taken at room temperature. The diffuse scattering on a sphere tangential to the reciprocal (001) and (110) planes respectively, are shown in Figs. 1(a) and 4(a). The relative size of the Ewald sphere and the reciprocal lattice is shown in Fig. 5.

For a direct comparison we have computed the scattering intensity corresponding to the experimental situation in Figs. 1(a) and 4(a); the results are shown in Figs. 1(b) and 4(b). In comparing computed and experimental data one has to keep in mind, that the latter data contain incoherent Compton scattering, and scattering in air, particularly noticeable in the central region of Fig. 4(a), due to the fact that the thin rodlike sample did not completely block the primary beam.

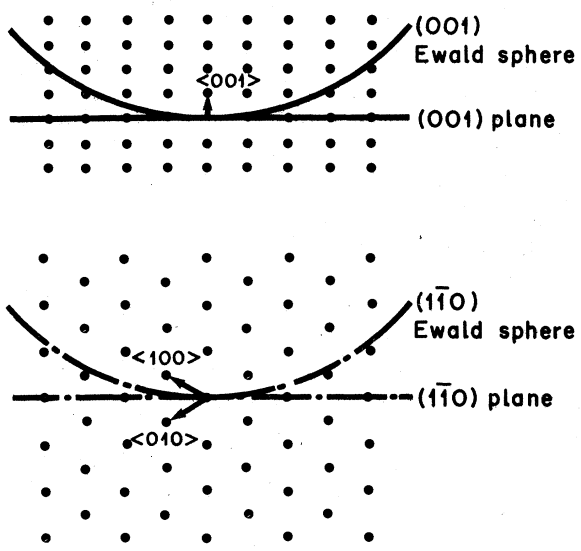

FIG. 5. Geometry of the reciprocal space of β-AgI. The side (top) and ground (bottom) view of the reciprocal lattice illustrate the relative size of the lattice and the Mo $K\alpha$ Ewald spheres corresponding to the experimental data in Figs. 1(a) and 4(a).

With low-frequency dispersionless lattice modes one has in principle to expect an appreciable second and higher phonon scattering. The calculation of these contributions is very time consuming and would have exceeded the capacity of our computational facilities; it appears, however, that these higher-order effects do not significantly contribute to the observed diffuse structures, as all observed structural elements are contained in the calculated one-phonon scattering.

We feel that the visual comparison represents an adequate proof of the thermal origin of the observed diffuse scattering and thus refrain from any complex numeric data comparison. The computation permits an identification of the phonon branches responsible for the diffuse scattering. As to be expected, most of the intensity originates from the low-frequency modes found in the analysis of the neutron scattering data. We illustrate this in Fig. 6 where we present the relevant phonon dispersion for a trace through the spherical cut in reciprocal space shown in Fig. 1. The cut is chosen so as to cross some of the most pronounced diffuse structures far from Bragg spots; the relevant phonon vectors $\vec{q}$ according to (3) along this trace lie on a rather arbitrary trace within the first Brillouin zone. Figure 6 displays the band of four branches close to 20 cm^{-1}, it further shows the total diffuse scattering along this trace as well as the small structureless portion of the intensity not originating from the low-frequency states.

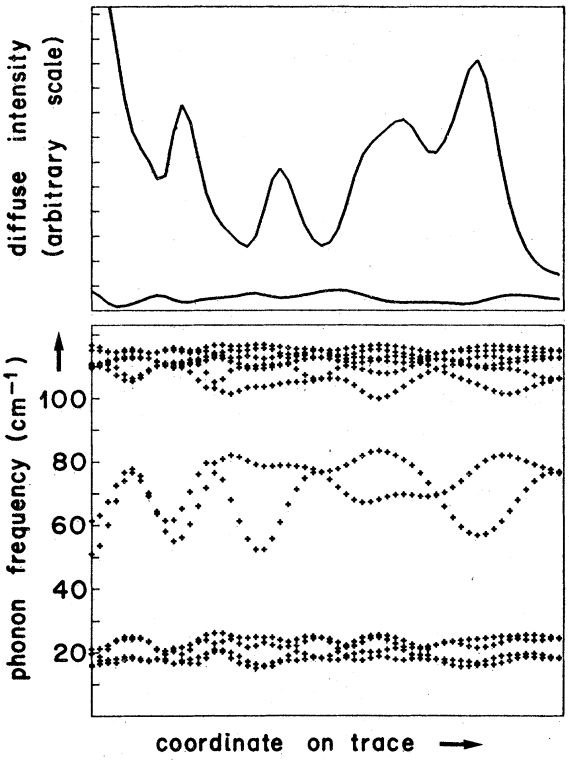

FIG. 6. (a) (Top) Computed total thermal scattering along the trace shown on Fig. 1(b) (not including absorption). The lower trace represents the contribution of the eight upper phonon branches, the major part of the scattering is thus due to the flat fourfold band of phonon states at about 20 cm^{-1}. (b) (Bottom) Relevant phonon dispersion along the trace shown in Fig. 1(b). Due to the spherical nature of this trace the corresponding phonon vectors $\vec{q}$ lie on a rather complex trace in the first Brillouin zone. The dispersion evidences the separation of the phonon states into a (fourfold) flat low-frequency band, a (twofold) longitudinal acoustical branch and a sixfold optical band.

VI. DISCUSSION, RELEVANCE FOR SUPERIONIC CONDUCTORS

The phase transition of silver iodide at 146 °C is mainly driven by the drastic increase of disorder entropy of the silver sublattice.[31] Raman measurements confirm that the low-frequency modes are more or less temperature independent, and that these are thus not soft modes driving the transition, although their eigenvectors are intimately related to the ionic displacements occurring in the β–α transition.[24] There is evidence that related low-frequency modes also exist in the α phase[31,32]; the existence of quasilocalized low-frequency modes may be a rather common feature of superionic conductors.

One may note the overall ringlike structures of the thermal diffuse scattering in β-AgI from Figs. 2 and 3. This structure is clearly evident in the diffuse background of the powder diffraction spectrum of β-AgI.[33] A detailed analysis shows that such a pattern is characteristic of vibrations in which only a few interionic distances are coherently modulated, i.e., characteristic of local modes. In fact a narrow flat band of phonon states is equivalent to noninteracting local Einstein oscillators. The structure of the diffuse background of the powder spectra does not change appreciably when going from the β to the α phase. In the disordered α phase this diffuse scattering has been interpreted in terms of a static pair-correlation function between the silver ions.[34] From our results we conclude that also in the α phase a large part of the diffuse scattering is of thermal nature originating from the large number of low-frequency lattice excitations indicated by computer simulations of the dynamics of the α phase[32] and by neutron diffraction experiments.[35]

VII. CONCLUSIONS

In the case of β-AgI we have explored the complex relationship between lattice dynamics and thermal diffuse x-ray scattering. As a result a very intense richly structured scattering pattern could be traced back to its lattice-dynamical origin. The physical cause of the strong diffuse scattering is the existence of low-frequency lattice modes whose frequency is determined by weak bending forces. As such modes appear to be typical for quite a few superionic conductors, we conclude that phonon scattering may mask the diffuse scattering due to a static short-range order so that it may in many cases be impossible to deduce any information about the latter from diffuse x-ray scattering.

[1]I. Waller, dissertation (Uppsala, 1925) (unpublished).
[2]J. Laval, C. R. Acad. Sci. Paris 207, 169 (1938).
[3]M. Born, Rep. Prog. Phys. 9, 294 (1942).
[4]Z. W. Wilchinsky, J. Appl. Phys. 15, 806 (1944).
[5]H. Lambot, Rev. Metall. 47, 709 (1950).
[6]A. Guinier, Bull. Soc. Fr. Mineral. Crystallogr. 77, 680 (1954).
[7]R. Moret, M. Huber, and R. Comès, Phys. Status Solidi A 38, 695 (1976).
[8]R. Comès, N. Lambert, H. Launois, and H. R. Zeller,

Phys. Rev. B 8, 571 (1973).
[9]F. Denoyer, R. Comès, A. F. Garito, and A. J. Heeger, Phys. Rev. Lett. 35, 445 (1975).
[10]Y. Le Cars, R. Comès, L. Dechamps, and J. Théry, Acta Cryst. A 30, 305 (1974).
[11]D. B. McWhan, S. J. Allen, J. P. Remeika, and P. D. Dernier, Phys. Rev. Lett. 35, 953 (1975).
[12]T. Hibma, H. U. Beyeler, and H. R. Zeller, J. Phys. C 9, 169 (1976).
[13]J. P. Boilot, G. Collin, R. Comès, J. Théry, R. Collongues, and A. Guinier, *Superionic Conductors*, edited by G. D. Mahan, and W. L. Roth (Plenum, New York, 1976).
[14]H. U. Beyeler, Phys. Rev. Lett. 37, 1557 (1976).
[15]H. U. Beyeler, L. Pietronero, S. Strässler, and H. J. Wiesmann, Phys. Rev. Lett. 38, 1532 (1977).
[16]D. B. McWhan, P. D. Dernier, C. Vettier, A. S. Cooper, and J. P. Remeika, Phys. Rev. B 17, 4043 (1978).
[17]For a general review see, *Superionic Conductors*, edited by G. D. Mahan and W. L. Roth (Plenum, New York, 1976).
[18]H. U. Beyeler, L. Pietronero, and S. Strässler (unpublished).
[19]J. C. Wang, M. Gaffari, and S. Choi, J. Chem. Phys. 63, 772 (1975).
[20]D. B. McWhan, S. M. Shapiro, J. P. Remeika, and G. Shirane, J. Phys. C 8, L487 (1975).
[21]W. Y. Hsu, Phys. Rev. B 14, 5161 (1976).
[22]P. Brüesch, H. U. Beyeler, and W. Bührer, in *Lattice Dynamics*, edited by M. Balkanski (Flammarion, Paris, 1978), p. 527.
[23]G. Burley, Amer. Mineral. 48, 1266 (1963).
[24]W. Bührer and P. Brüesch, Solid State Commun. 16, 155 (1975).
[25]W. Bührer, R. M. Nicklow, and P. Brüesch, Phys. Rev. B 17, 3362 (1978).
[26]L. W. Strock, Z. Phys. Chem. B 25, 411 (1934); B 31, 132 (1936).
[27]W. Bührer and W. Hälg, Helv. Phys. Acta 47, 27 (1974).
[28]R. J. Cava, F. Reidinger, and B. J. Wuensch, Solid State Commun. 24, 411 (1977).
[29]T. Hibma (private communication).
[30]W. Cochran and R. A. Cowley, in *Handbuch der Physik*, edited by S. Flügge (Springer, Berlin, 1967), p. 59.
[31]H. U. Beyeler, P. Brüesch, L. Pietronero, W. R. Schneider, S. Strässler, and H. R. Zeller, Springer Tracts Mod. Phys. (to be published).
[32]R. Alben and G. Burns, Phys. Rev. B 16, 3746 (1977).
[33]H. U. Beyeler (unpublished).
[34]M. Suzuki and H. Okazaki, Phys. Status Solidi A 42, 133 (1977).
[35]W. Bührer and P. Brüesch (unpublished).

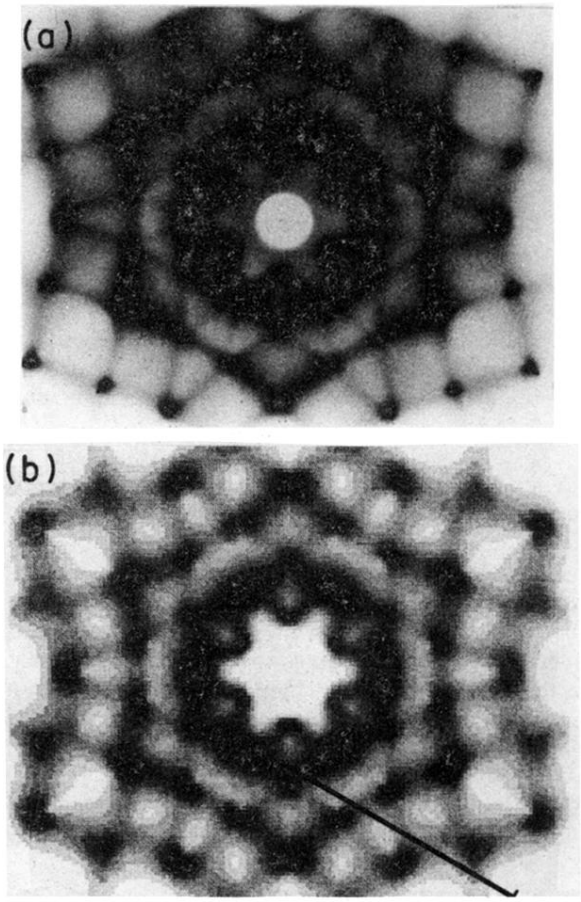

FIG. 1. (a) (Top) experimental diffuse scattering in β-AgI. The picture is taken in a steady-crystal–steady-film geometry (monochromatic *Laue* set up) with the incident beam perpendicular to the hexagonal basal plane. The scattering intensity thus corresponds to that on a sphere tangential to the reciprocal basal plane [(001) Ewald sphere] as shown in Fig. 5. The scattering on the trace in the lower left side is analyzed in Fig. 6. (b) (Bottom) Computed thermal diffuse scattering intensity in the geometry of Fig. 1(a). The scattering is displayed on a 16-step gray scale. The data are corrected for absorption according to the experimental situation of Fig. 1(a).

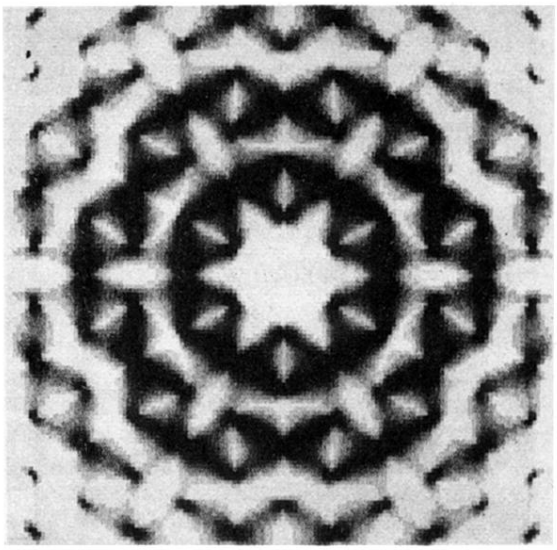

FIG. 2. Computed thermal diffuse scattering in the reciprocal basal plane of β-AgI. The data do not contain the (infinitely sharp) Bragg reflexions, but their position is evidenced by the diffuse haloes due to the long-wavelength acoustical phonons.

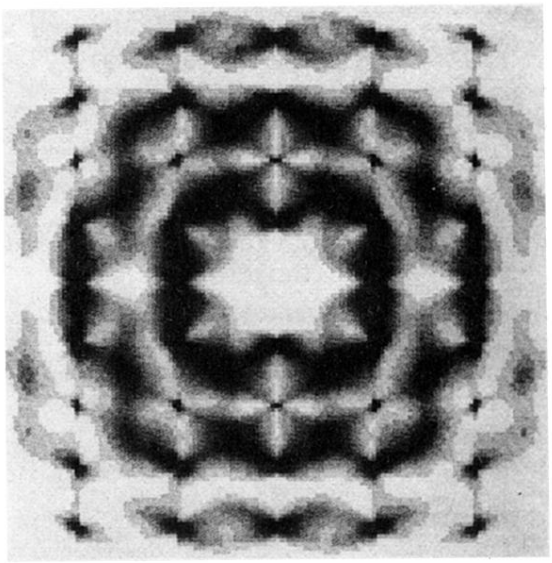

FIG. 3. Computed thermal diffuse scattering in the reciprocal $(1\bar{1}0)$ plane.

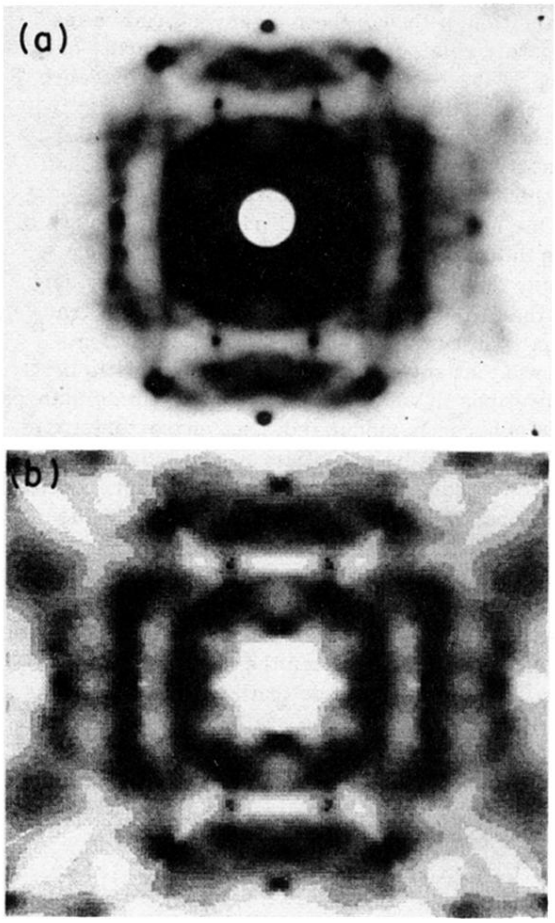

FIG. 4. (a) (Top) Experimental diffuse scattering on a sphere tangential to the reciprocal $(1\bar{1}0)$ plane [$(1\bar{1}0)$ Ewald sphere]; as thin rodlike samples had to be used in this geometry, the central part of the picture contains an appreciable amount of air scattering from the primary beam. (b) (Bottom) Computed thermal diffuse scattering in the geometry of Fig. 4(a).